

Photorefractive properties of undoped lithium tantalate crystals for various composition

F. Holtmann,^{a)} J. Imbrock, Ch. Bäumer, H. Hesse, and E. Krätzig
Physics Department, University of Osnabrück, D-49069 Osnabrück, Germany

D. Kip

Institute of Physics, Technical University of Clausthal, D-38678 Clausthal-Zellerfeld, Germany

(Received 15 March 2004; accepted 16 August 2004)

Lithium tantalate crystals of compositions ranging from 48.3 mol % to 50.0 mol % lithium oxide are fabricated by vapor transport equilibration. Light-induced refractive index changes of the crystals are investigated with holographic methods at usual cw-laser intensities ($\approx 10^5$ W/m²) and with a single focused laser beam at high light intensities up to 2×10^7 W/m². In stoichiometric crystals the index changes are reduced by more than two orders of magnitude when compared with congruently melting ones. Simultaneously, the normalized photoconductivity σ_{ph}/I , where I is the light intensity, increases by nearly two orders of magnitude. Therefore, stoichiometric lithium tantalate is an attractive material for applications such as frequency conversion via quasi-phase matching. © 2004 American Institute of Physics. [DOI: 10.1063/1.1805189]

I. INTRODUCTION

Lithium tantalate (LiTaO₃) crystals are of special interest for applications such as frequency conversion via quasi-phase matching in periodically poled crystals.^{1,2} In this context light-induced refractive index changes, also known as optical damage, are of great disadvantage. This disturbing effect is caused by both, extrinsic and intrinsic defects which initiate the development of space charge fields that finally change the material's refractive index. Extrinsic defects can be minimized by the use of very pure starting chemicals for crystal growth. On the other hand, the reduction of intrinsic defects is more difficult. The congruently melting composition of LiTaO₃ [about 48.5 mol % Li₂O (Ref. 3)] does not coincide with the stoichiometric one (50.0 mol % Li₂O). Because of the Li deficit, congruent LiTaO₃ crystals possess a large number of intrinsic defects such as Li vacancies and Ta_{Li} antisite defects (Ta on Li site). Besides optical damage many physical properties of LiTaO₃ crystals depend on the Li content, such as coercive field, birefringence, Curie temperature, and position of the absorption edge.⁴

A reduction of intrinsic defects can be realized by several methods. The crystals can be doped by adding MgO to the melt,⁵ where Mg ions occupy Li sites in the crystal thus reducing the number of Ta_{Li} antisite defects. Alternatively, nearly stoichiometric crystals can be grown from a melt containing an excess of Li by the double crucible Czochralski method.^{3,6} A third method, the vapor transport equilibration (VTE) process, is a postgrowth treatment.⁷ Here, LiTaO₃ crystals are annealed together with a LiTaO₃ powder of a certain composition until equilibrium is reached.

In this paper we investigate light-induced refractive index changes in LiTaO₃ crystals in dependence of composition. Therefore, we have prepared several samples of different Li concentrations using VTE treatments. For the

measurements we either use a holographic setup at usual cw-laser intensities ($\approx 10^5$ W/m²), or a single focused laser beam that provides high light intensities up to 2×10^7 W/m².

II. EXPERIMENTAL METHODS

A. Samples

Several samples of different compositions in the range from 48.3 to 50.0 mol % Li₂O are prepared using VTE treatments. Starting crystals for VTE processing are obtained from Czochralski-grown boules of the congruently melting composition. The boules are cut into plates of 0.3–0.5 mm thickness. A VTE treatment is carried out by heating the crystals in a platinum crucible together with a powder of LiTaO₃ of a certain composition. Annealing takes place at a temperature of 1200 °C for a duration of 140 h. A detailed description of this VTE treatment is given in an earlier paper.⁴ In order to determine the Li content of the powder, an accurate weight control is carried out during the whole procedure. Thus it is possible to determine the evaporation losses of Li₂O and an absolute accuracy for the composition of ± 0.05 mol % is achieved. The lithium concentrations given in the following are the concentrations of the powder after annealing. Below 50.0 mol % Li₂O this concentration is equal to the concentration of the treated crystals in the equilibrium state, whereas for concentrations higher than 50.0 mol % Li₂O in the powder it can be assumed that a maximum value of 50.0 mol % Li₂O is obtained in the crystals.⁴ For further investigations the crystals are polished to optical quality. Poling is achieved by heating the crystals to a temperature of 750 °C (above Curie temperature) and cooling down quickly with an applied electric field of 30 V/cm.

^{a)}Electronic address: frank_holtmann@web.de

B. Holography

Holographic measurements are performed with a two-beam interference setup as described, e.g., in Ref. 8. Two beams of an Ar⁺ ion laser with a wavelength of $\lambda=488$ nm are superimposed inside the crystal. The intensity can be controlled by means of a combination of a $\lambda/2$ -plate and a polarizer. A maximum intensity of 1.6×10^5 W/m² can be reached and the recording light is ordinarily polarized. The interference pattern has a fringe spacing of $\Lambda=0.8$ μ m and the grating vector K is directed parallel to the crystal's c axis. The resulting refractive index grating can be probed by a weak beam of a He-Ne laser ($\lambda=633$ nm) that is Bragg-matched and extraordinarily polarized. The intensities of the transmitted (I_t) and the diffracted (I_d) beams are measured by photodiodes. For this measurement, the samples are mounted in front of an aperture with a diameter of 1 mm. With the diffraction efficiency η given by

$$\eta = \frac{I_d}{I_d + I_t}, \quad (1)$$

the refractive index changes Δn_e (extraordinary polarization) can be determined using Kogelnik's formula⁹

$$\Delta n_e = \frac{\lambda \cos \Theta}{\pi d} \arcsin(\sqrt{\eta}). \quad (2)$$

Here λ denotes the wavelength of the probe laser, d is the thickness of the crystal, and Θ is the Bragg angle inside the crystal. With a third laser beam ($\lambda=488$ nm, ordinarily polarized) holograms can be erased off-Bragg. The temporal development of the refractive index changes Δn_e during the recording procedure and the temporal decay during erasure of the refractive index changes follow monoexponential laws:

$$\Delta n_e = \Delta n_e^S [1 - \exp(-t/\tau)] \quad \text{for recording}, \quad (3)$$

$$\Delta n_e = \Delta n_e^S \exp(-t/\tau) \quad \text{for erasure}. \quad (4)$$

The saturation value of refractive index changes is denoted by Δn_e^S and the recording time constant by τ . This time constant yields the photoconductivity $\sigma_{\text{ph}} = \epsilon_{33} \epsilon_0 / \tau$ with the dielectric constant $\epsilon_{33} = 43.4$ (Ref. 10) and the permittivity ϵ_0 of free space. In order to provide a stable setup even for long writing processes an active stabilization is used. One of the interfering beams is phase-modulated by a piezoelectrically driven mirror with a frequency much higher than the frequency response of the crystal. Using a lock-in amplifier the first (I^Ω) and second harmonics ($I^{2\Omega}$) are extracted from the detected intensity of one of the beams behind the sample. With the assumption that the bulk photovoltaic effect dominates the charge transport, the second harmonic approaches zero. Hence $I^{2\Omega}$ can be used as an error signal and as control variable for a feedback loop acting on the piezoelectrically supported mirror.¹¹⁻¹³

C. Single-beam setup

For the investigation of light-induced refractive index changes at high light intensities up to 2×10^7 W/m² a single-beam setup is used (Sénarmont com-

pensator). The extraordinarily polarized beam of an Ar⁺ ion laser at a wavelength $\lambda=488$ nm is focused by a lens to a diameter ($1/e^2$) D of ≈ 80 μ m and collimated to the sample. The intensity of this pump beam can be controlled by a combination of $\lambda/2$ -plate and polarizer. The light-induced changes of the birefringence are determined by a weak He-Ne laser beam ($\lambda=633$ nm) which is focused roughly to half of the diameter of the pump beam. In order to bring the pump beam and the test beam into the same direction, both beams are superimposed by the use of a nonpolarizing beam splitter. The polarization of the test beam is oriented at an angle of 45° towards the optical axis of the sample (c axis) which is situated in the plane perpendicular to the wave vectors of the test and pump beam. Inside the crystal the incident wave is split into an ordinary (with n_o) and an extraordinary wave (with n_e) due to birefringence. These two waves possess different phase velocities, i.e., the superposition results in an elliptically polarized beam. Behind the crystal a $\lambda/4$ -plate is introduced at an angle of $\pm 45^\circ$ with respect to the c axis to get linearly polarized light. Depending on the natural birefringence of the crystal the polarization of the incident light is rotated and a second polarizer is adjusted to block this probe light completely.

A light-induced change of the birefringence $\delta \Delta n$ leads to an additional rotation of the polarization of the probe light. The intensity I_T behind the second polarizer is given by

$$I_T = I_0 \sin^2 \left(\frac{\pi d \delta \Delta n}{\lambda} \right). \quad (5)$$

Assuming that the temporal behavior of the light-induced birefringence changes follows Eq. (3) we obtain the time dependence of the intensity behind the second polarizer,

$$I_T(t) = I_0 \sin^2 \left\{ \frac{\pi d \delta \Delta n^S [1 - \exp(-t/\tau)]}{\lambda} \right\}. \quad (6)$$

Here $\delta \Delta n^S$ is the saturation value of the light-induced birefringence change and the time constant τ yields again the photoconductivity $\sigma_{\text{ph}} = \epsilon_{33} \epsilon_0 / \tau$. After each measurement the samples are heated to 300 $^\circ$ C for half an hour to erase the generated refractive index changes completely.

III. EXPERIMENTAL RESULTS

A. Holographic measurements

In our holographic measurements all samples show a monoexponential time dependence of the light-induced refractive index changes as described by Eqs. (3) and (4). In Fig. 1 the saturation value of refractive index changes Δn_e^S is plotted versus the Li content of the powder after the VTE treatment. The measurements have been performed at an intensity of 1.6×10^5 W/m². Up to a Li concentration of 49.5 mol % Li₂O Δn_e^S exceeds 1×10^{-4} . For Li concentrations larger than 49.5 mol % Δn_e^S decreases rapidly and above 50.0 mol % Li₂O no refractive index changes can be observed. The detection limit of light-induced refractive index changes measured with a holographic setup is $\Delta n_e^S \approx 2 \times 10^{-6}$.

Our measurements show that the photoconductivity σ_{ph} is proportional to the light intensity I . The normalized pho-

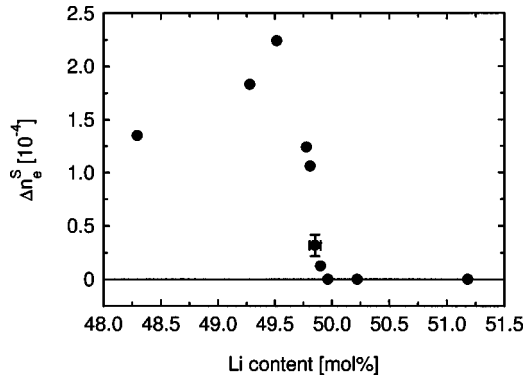


FIG. 1. Saturation value of refractive index changes Δn_e^S ($\lambda=633$ nm, light intensity $I=1.6 \times 10^5$ W/m²) vs lithium content of the powder after a VTE treatment. Li concentrations of the powder larger than 50.0 mol % lead to Δn_e^S values smaller than 2×10^{-6} .

toconductivity σ_{ph}/I increases from 7×10^{-19} m/V² for a sample with a Li concentration of 48.3 mol % to 4×10^{-17} m/V² for a sample with 49.9 mol % Li₂O (Fig. 2). For samples treated with a powder containing more than 50.0 mol % Li₂O the photoconductivity cannot be determined from holographic measurements because no refractive index changes are observed.

B. Single-beam measurements

The following measurements are based upon the generation of birefringence changes $\delta(\Delta n) = \Delta n_e - \Delta n_o$ by a focused laser beam and detection of these changes by another weak beam which is focused to a smaller diameter. In order to examine the transverse profile of the induced birefringence changes we first illuminate the sample (49.2 mol % Li₂O) with the pump beam for a few minutes. Then the pump beam is switched off and the sample is shifted perpendicular to the probe beam in a transverse direction either parallel or perpendicular to the *c* axis of the crystal and the intensity behind the second polarizer is detected (Fig. 3). As can be seen, the measurements show Gaussian shapes of similar widths.

In the following measurements the samples are illuminated by the pump beam while the saturation values of light-induced birefringence changes $\delta\Delta n^S$ and the time constants τ

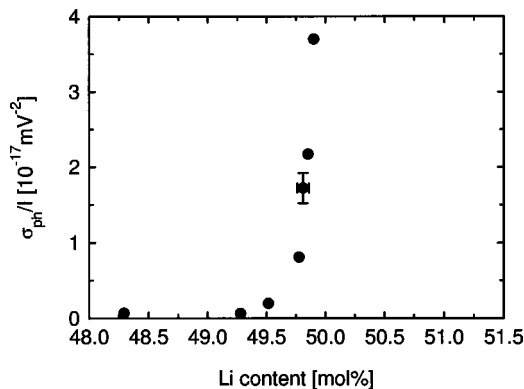


FIG. 2. Photoconductivity σ_{ph} ($\lambda=488$ nm) normalized to light intensity I (1.6×10^5 W/m²) vs lithium content of the powder after VTE treatments. For a lithium content larger than 50.0 mol % no index changes and therefore no photoconductivity can be measured.

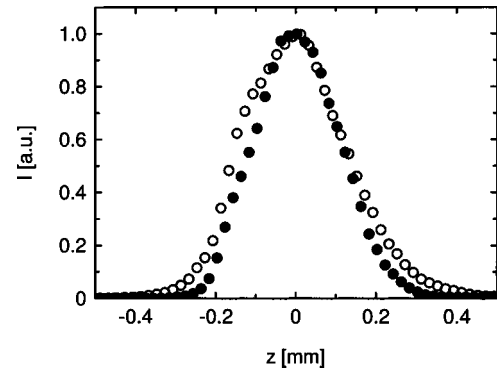


FIG. 3. Intensity of probe light behind the second polarizer as a function of the position of the sample (49.2 mol % Li₂O) shifted in a plane perpendicular to the beam after illumination with the pump beam for a few minutes (pump beam: wavelength $\lambda=488$ nm, intensity $I=10^7$ W/m², diameter $D=80$ μ m; test beam: $\lambda=633$ nm, $I \approx 6 \times 10^4$ W/m², $D=40$ μ m). The sample is shifted parallel (●) and perpendicular (○) to the *c* axis. For zero shift the maximum intensity is obtained.

are determined with the probe beam. In Fig. 4 the saturation value $\delta\Delta n^S$ is plotted versus pump light intensity for four samples with different Li contents. The intensity dependence of $\delta\Delta n^S$ can be described by a function of the form $\delta\Delta n_{\infty}^S I / (b + I)$, with $\delta\Delta n_{\infty}^S$ as the maximum value of the saturation birefringence changes and *b* as the intensity where half of the maximum value of $\delta\Delta n_{\infty}^S$ is reached. The maximum value depends on the Li content of the sample and decreases considerably with increasing lithium concentration (Fig. 5). For samples treated with a powder containing more than 50.0 mol % Li₂O no changes of birefringence can be observed even for the highest possible intensities of about 2×10^7 W/m². The detection limit of light-induced birefringence changes measured with a single-beam setup is $\delta\Delta n^S \approx 5 \times 10^{-5}$.

From the temporal behavior of the light-induced birefringence changes the photoconductivity can be determined. Over the whole range of the used intensities the intensity dependence of the photoconductivity can be approximated by a linear relation (Fig. 6). The dependence of σ_{ph} on the Li content is presented in Fig. 7. The change of the normalized photoconductivity σ_{ph}/I with Li concentration is the same as

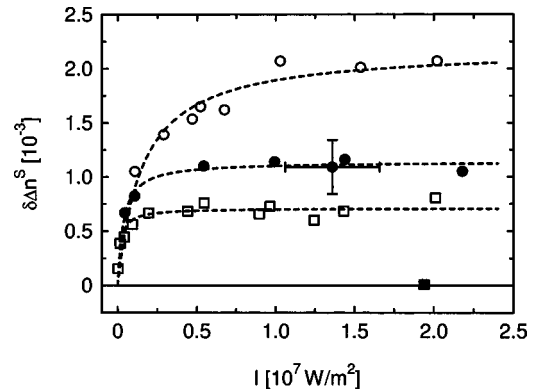


FIG. 4. Saturation values of light-induced birefringence changes $\delta\Delta n^S$ vs pump light intensity I . The Li content of the powder after the VTE treatment was 49.2 mol % (○), 49.8 mol % (●), 49.9 mol % (□) and 51.2 mol % (■). The dashed lines are fits according to $\delta\Delta n^S = \delta\Delta n_{\infty}^S I / (b + I)$.

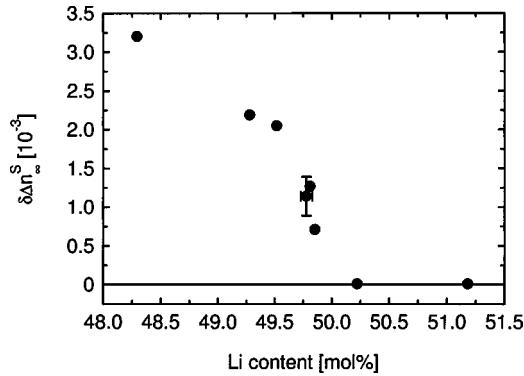


FIG. 5. Maximum value of saturation birefringence changes $\delta\Delta n_{\infty}^S$ vs the lithium content of the powder. For a Li content larger than 50.0 mol % no light-induced birefringence changes are detected ($\delta\Delta n^S < 5 \times 10^{-5}$).

that measured for low intensities with the holographic methods. Congruently melting samples have a much lower photoconductivity than lithium rich ones. Samples treated with a powder containing more than 50.0 mol % Li_2O show no detectable light-induced birefringence changes and the photoconductivity cannot be determined in these samples.

IV. DISCUSSION

The holographic measurements performed at intensities of about $1.6 \times 10^5 \text{ W/m}^2$ yield relatively large light-induced refractive index changes Δn_e^S of about 10^{-4} for our undoped LiTaO_3 crystals with < 49.5 mol % Li_2O . For larger Li concentrations the Δn_e^S values decrease with increasing Li concentration and above 50.0 mol % Li_2O in the powder no refractive index changes can be observed (Fig. 1). On the other hand, the normalized photoconductivity σ_{ph}/I increases by two orders of magnitude for Li concentrations larger than 49.5 mol % Li_2O (Fig. 2). This points to a reciprocal behavior of light-induced refractive index change and photoconductivity.

For the single-beam measurements we have examined the shape of light-induced refractive index changes by detecting the intensity behind the second polarizer while shifting the sample in a plane perpendicular to the beam (Fig. 3). When we shift the sample perpendicular to the c axis we observe the expected Gaussian shape.¹⁴ For a movement par-

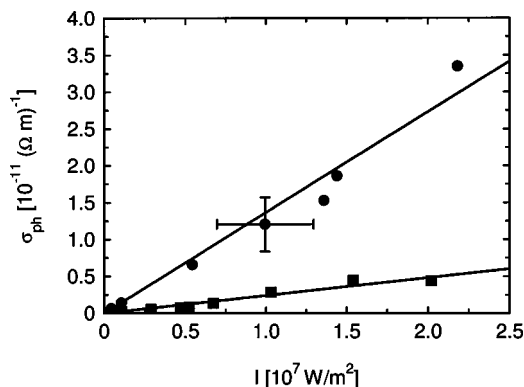


FIG. 6. Photoconductivity σ_{ph} vs pump light intensity for two samples containing 49.8 mol % (●) and 49.2 mol % Li_2O (■), respectively. The solid lines are linear fits.

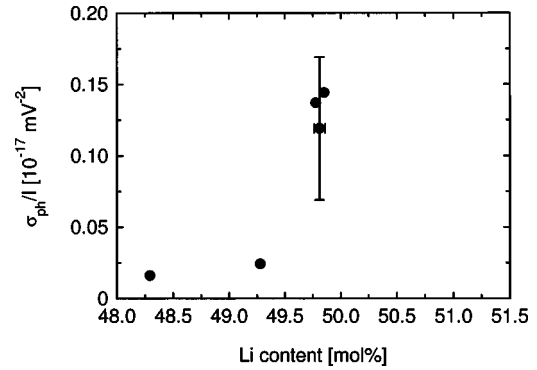


FIG. 7. Normalized photoconductivity σ_{ph}/I vs Li content of the powder after VTE treatments.

allel to the c axis we also obtain a Gaussian shape, though one expects a main maximum and two side maxima.¹⁴ Obviously the resolution of our method is not sufficient to observe the side maxima for our thin samples (thickness only 0.3–0.5 mm) in agreement with observations for LiNbO_3 .¹⁵

The saturation values of light-induced birefringence changes $\delta\Delta n_{\infty}^S$ increase with increasing light intensity and reach a saturation value $\delta\Delta n_{\infty}^S$ for high intensities (Fig. 4). The dependence of $\delta\Delta n_{\infty}^S$ on the Li concentration exhibits a similar behavior as the light-induced refractive index changes Δn_e^S determined from holographic measurements at low intensities. The $\delta\Delta n_{\infty}^S$ values decrease with increasing Li content of the powder and above 50.0 mol % Li_2O no birefringence changes can be observed (Fig. 5). The maximum saturation value $\delta\Delta n_{\infty}^S$ at 10^7 W/m^2 for a certain Li concentration is about one order of magnitude larger than the corresponding Δn_e^S value determined from holographic measurements at about 10^5 W/m^2 . The photoconductivity values obtained from single-beam measurements also increase considerably with increasing Li content (Fig. 7).

The dependences of the photoconductivity as well as of the light-induced changes of the refractive index and of birefringence on the Li concentration may be explained qualitatively by considering the charge transport that is similar to the charge transport in LiNbO_3 crystals.¹⁶ LiTaO_3 crystals of the congruently melting composition contain a large number of intrinsic defects, among them Ta^{5+} ions on Li^+ sites ($\text{Ta}_{\text{Li}}^{5+}$). Under illumination electrons of filled deep traps (which are always present as impurities), e.g., Fe^{2+} or Cu^+ ions, can be transferred to $\text{Ta}_{\text{Li}}^{5+}$ ions forming $\text{Ta}_{\text{Li}}^{4+}$ polarons.¹⁷ From these polarons as well as from filled deep traps electrons can be optically excited to the conduction band. The photoconductivity σ_{ph} resulting from excited electrons is given by

$$\sigma_{\text{ph}} = e\mu N_e, \quad (7)$$

where e denotes the electron charge, μ the mobility, and N_e the density of excited electrons in the conduction band. With increasing Li content the number of $\text{Ta}_{\text{Li}}^{5+}$ antisite defects decreases influencing mobility μ and electron density N_e .

In LiTaO_3 the dominating charge driving force is the photovoltaic effect.¹⁸ Then the space charge field E_{SC} can be approximated by

$$E_{SC} \propto \frac{\beta_D^* I N_D}{\sigma_{ph}} + \frac{\beta_X^* I N_X}{\sigma_{ph}}. \quad (8)$$

Here β_D^* and β_X^* denote the specific photovoltaic constants of deep and shallow traps, respectively, N_D is the concentration of filled deep traps and N_X the concentration of filled shallow traps (Ta_{Li}^{4+}). With increasing Li content σ_{ph} increases and N_X decreases leading to a decrease of E_{SC} .¹⁹ Thus light-induced refractive index changes and birefringence changes decrease, too. It is also possible that β_X^* depends on the Li concentration and that some extrinsic impurity ions diffuse out of the crystal during the VTE treatments. For crystals that have been treated with a powder containing more than 50.0 mol % Li_2O , no changes could be detected.

V. CONCLUSIONS

We have prepared $LiTaO_3$ crystals of different compositions in the range from 48.3 to 50.0 mol % using VTE treatments. The saturation values of light-induced refractive index and birefringence changes increase with increasing intensity up to a maximum value at high light intensities. With increasing Li content these maximum values decrease and for stoichiometric samples no optical damage is observed even at intensities up to 2×10^7 W/m². The decrease is correlated with a strong increase of photoconductivity. Therefore, VTE-treated stoichiometric $LiTaO_3$ is an attractive material for applications such as frequency conversion in periodically poled crystals via quasi-phase matching.

ACKNOWLEDGMENT

Financial support of the Bundesministerium für Bildung und Forschung (Grant No. 13N8076) is gratefully acknowledged.

- ¹M. M. Fejer, G. A. Magel, D. H. Jundt, and R. L. Byer, *IEEE J. Quantum Electron.* **28**, 2631 (1992).
- ²K. Mizuuchi and K. Yamamoto, *J. Appl. Phys.* **72**, 5061 (1992).
- ³Y. Furukawa, K. Kitamura, E. Suzuki, and K. Niwa, *J. Cryst. Growth* **197**, 889 (1999).
- ⁴C. Bäumer, C. David, A. Tunyagi, K. Betzler, H. Hesse, E. Krätzig, and M. Wöhlecke, *J. Appl. Phys.* **93**, 3102 (2003).
- ⁵F. Nitanda, Y. Furukawa, S. Makio, M. Sato, and K. Ito, *Jpn. J. Appl. Phys., Part 1* **34**, 1546 (1995).
- ⁶K. Kitamura, Y. Furukawa, K. Niwa, V. Gopalan, and T. E. Mitchell, *Appl. Phys. Lett.* **73**, 3073 (1998).
- ⁷P. F. Bordui, R. G. Norwood, D. H. Jundt, and M. M. Fejer, *J. Appl. Phys.* **71**, 875 (1992).
- ⁸J. Imbrock, A. Wirp, D. Kip, E. Krätzig, and D. Berben, *J. Opt. Soc. Am. B* **19**, 1822 (2002).
- ⁹H. Kogelnik, *Bell Syst. Tech. J.* **48**, 2909 (1969).
- ¹⁰R. T. Smith and F. S. Welsh, *J. Appl. Phys.* **42**, 2219 (1971).
- ¹¹P. A. M. dos Santos, L. Cescato, and J. Frejlich, *Opt. Lett.* **13**, 1014 (1988).
- ¹²P. M. Garcia, K. Buse, D. Kip, and J. Frejlich, *Opt. Commun.* **117**, 235 (1995).
- ¹³S. Breer, K. Buse, K. Peithmann, H. Vogt, and E. Krätzig, *Rev. Sci. Instrum.* **69**, 1591 (1998).
- ¹⁴F. S. Chen, *J. Appl. Phys.* **40**, 3389 (1969).
- ¹⁵O. Althoff and E. Krätzig, *Proc. SPIE* **1273**, 12 (1990).
- ¹⁶F. Jermann and J. Otten, *J. Opt. Soc. Am. B* **10**, 2085 (1993).
- ¹⁷J. Imbrock, S. Wevering, K. Buse, and E. Krätzig, *J. Opt. Soc. Am. B* **16**, 1392 (1999).
- ¹⁸A. M. Glass, D. von der Linde, and T. J. Negran, *Appl. Phys. Lett.* **25**, 233 (1974).
- ¹⁹M. Jazbinšek, M. Zgonik, S. Takekawa, M. Nakamura, K. Kitamura, and H. Hatano, *Appl. Phys. B: Lasers Opt.* **75**, 891 (2002).